Ḥadashot Arkheologiyot—
Excavations and Surveys in Israel 133

Appendix: Analysis of Plaster from the Winepress Complex at Tel Yavne

Ifat Shapira and Yotam Asscher

Introduction

The large, Persian-period winepress complex (350 sq m; Sub-Areas A2 and A4) uncovered at Tell Yavne comprises 14 treading floors and 24 collecting vats, all plastered. The vats, some of which included niches, exhibited some variation, and were thus divided into seven morphological types: rectangular with a shallow niche (Vats A, B; Fig. 1:1); shallow round (Vats C, D, Y; Fig. 1:2); deep round (Vats E–G, N; Fig. 1:3); shallow rectangular (Vats I–K; Fig. 1:4); square with a deep niche (Vats L, M; Fig. 1:5); square with a shallow niche (Vats T–X; Fig. 1:6); and square (Vats O–S; Fig. 1:7). All these vats, except for Vat E, were in use in Stratum III; it seems likely that Vat E was first installed in Stratum IV, but its use continued in Stratum III.

The magnitude of this winepress complex from the Persian period is unique in Israel, and thus calls for a detailed examination with the aim of understanding the function of its components and the technology employed to construct them. Several analytical diagnostic tools were applied to the plaster of the winepress complex; both their binder component and their aggregates were examined. The study sought to determine the mineralogical and structural composition of the plaster coating in vats of the various types, as these may indicate differences in the function of the installations in which they were used.

This is a report of the preliminary results of analysis carried out on 26 samples of plaster, taken from 16 installations ascribed to Stratum III—7 treading floors and 9 vats, belonging to three different morphological types—and from two earlier vats ascribed to stratum IV (Table 1; each basket number represents a sample).

Methods

All 26 plaster samples were examined visually with the naked eye and underwent spectrographic analyses. One sample underwent a microscopic examination as well.

Microscopy.— A thin section of one sample, from a multilayered plaster coating a treading floor, was examined under a microscope to determine its micromorphology. The sample was embedded in


1


2


3


4


5


6


7

Fig. 1. Vat types: (1) Rectangular with a shallow niche; (2) shallow round; (3) deep round; (4) shallow rectangular; (5) square with a deep niche; (6) square with a shallow niche; (7) square.

epoxy resin, and after drying the surfaces of the hardened plaster it was polished down and glued to a microscope slide. The sample was cut, ground down and polished until a ~30 μm thin section remained (for a full description of the procedure of producing sediment thin sections, see Asscher and Goren 2016). The slide was examined with Polarized Light Microscopy using a Zeiss Axioscope 5.

Spectroscopy.— All 26 samples underwent Fourier Transform Infrared (FTIR) spectroscopy. This analysis provides information on the different chemical phases, both organic and inorganic, of the material, which characterize the mineralogical composition of inorganic materials. In order to generate infrared spectra, a one-gram sample is homogenized in an agate mortar. Approximately 0.2 mg is then ground to a fine powder and mixed with approximately 20 mg of KBr (FTIR-grade), and finally each sample is pressed into a 7-mm pellet using a hand press (PIKE Technologies). Infrared spectra were obtained using a Nicolet iS5 spectrometer at a 4 cm^{-1} resolution. Spectra were compared to the Kimmel Center for Archaeological Science Infrared Standards Library, Weizmann Institute of Science.

In the case of the plaster sample that had multiple visible layers, each layer was analyzed separately, with the aim of comparing the various layers. Differences between layers could be interpreted as a difference in either production technology, use, function, or chronology, i.e., belonging to different stratigraphic phases. On the other hand, similarities are understood as resulting from maintenance and the continued employment of a specific production procedure for a specific function. As the aggregates were found to be shells—a material which can be analyzed for exposure to heat during the production process—the binder and the aggregates in each of the samples were analyzed separately.

FTIR analysis can also be used to indicate the plaster's state of preservation by describing the atomic disorder of the calcitic binder when compared with modern standards of plaster (Regev et al. 2010). This is done by measuring the normalized heights of the V2 and V4 vibrational bands of the materials, following Regev et al. (2010). The binder is expected to have a higher atomic disorder in comparison with geological calcite, as it was exposed to higher temperatures during its production (Weiner 2010). Thus, when samples are disordered, it is assumed that they come from well-preserved plasters. However, if samples seem closer to geological materials, they either come from a badly preserved plaster or contain geological materials that were used as aggregates. Estimating the samples' state of preservation was done through a process known as Grinding Curves, in which the sample is measured several times following the regrinding of the pellet, thus decoupling the optical effect that interferes with the FTIR absorption spectrum (Poduska et al. 2011).

Table 1. Spectral Indicators of Samples from Area A (NA = Non-available)

Installation Type			Locus	Basket	Type of material	Sample provenance	Calcite\ Aragonite	v2	v4
Vats	Rectangular with a shallow niche	A	16079	160519	Binder	Wall	Calcite	359	77
			16079	160520	Binder	Wall	Calcite	343	66
			16079	160519	Aggregate	Wall	Aragonite	NA	NA
			16079	160520	Aggregate	Wall	Aragonite	NA (Non-available)	NA
		B	16024	160522	Binder	Wall	Calcite	409	90
			16024	160523	Binder	Floor	Calcite	419	101
			16024	160524	Binder	Wall	Calcite	363	73
			16024	160522	Aggregate	Wall	Aragonite	NA	NA
			16024	160523	Aggregate	Floor	Aragonite	NA	NA
			16024	160524	Aggregate	Wall	Aragonite	NA	NA
	shallow round	C	16112	160527	Binder	Wall	Calcite	361	67
			16112	160527	Aggregate	Wall	Calcite	NA	NA
			16112	160527/2	Aggregate	Wall	Aragonite	NA	NA
			16112	160527/3	Aggregate	Wall	Aragonite	NA	NA
			16112	160527/4	Aggregate	Wall	Aragonite	NA	NA
			16112	160527/5	Aggregate	Wall	Aragonite	NA	NA
		D	16021	160528	Binder	Wall	Calcite	409	97
			16021	160528	Binder	Wall	Calcite	378	92
			16021	160528	Aggregate	Wall	Calcite	NA	NA
			16021	160528	Aggregate	Wall	Calcite	NA	NA
		Y	16025	160525	Binder	Wall	Calcite	418	79
			16025	160526	Binder	Floor	Calcite	359	71
			16025	160525	Aggregate	Wall	Aragonite	NA	NA
			16025	160526	Aggregate	Floor	Aragonite	NA	NA
	square with a shallow niche	T	11062	110256	Binder	Wall	Calcite	341	54
			11141	110255	Binder	Wall	Calcite	353	67
			11141	110255	Binder	Wall	Calcite	338	68
			11062	110256	Aggregate	Wall	Aragonite	NA	NA
			11141	110255	Aggregate	Wall	Aragonite	NA	NA
		V	11008	110254	Binder	Wall	Calcite	388	66
			11008	110254	Aggregate	Wall	Aragonite	NA	NA
		W	11103	110253	Binder	Wall	Calcite	305	42
			11103	110253	Aggregate	Wall	Aragonite	NA	NA
		X	11007	110252	Binder	Wall	Calcite	329	57
			11007	110252	Aggregate	Wall	Aragonite	NA	NA
	Stratum IV (Iron Age–Persian)		11245	110666	Binder	Floor	Calcite	381	73
			11245	110666	Aggregate	Floor	Aragonite	NA	NA
			11148	110668	Binder	Floor	Calcite	394	69
			11248	110667	Binder	Floor	Calcite	409	77
			11148	110668	Aggregate	Floor	Aragonite	NA	NA
			11248	110667	Aggregate	Floor	Aragonite	NA	NA

Table 1. (cont.)

Installation Type		Locus	Basket	Type of material	Sample provenance	Calcite\ Aragonite	v2	v4
Treading floors	1	16061	160521	Aggregate	Wall	Aragonite	NA	NA
		16061	160521	Binder	Wall	Calcite	380	80
	2	16013	160059	Aggregate	Floor	Aragonite	NA	NA
		16013	160059	Aggregate	Floor	Aragonite	NA	NA
		16013	160059	Aggregate	Floor	Aragonite	NA	NA
		16013	160059	Binder	Floor	Calcite	361	62
		16013	160059	Binder	Floor	Calcite	339	73
		16013	160059	Binder	Floor	Calcite	373	65
	3	16001	160058	Aggregate	Floor	Aragonite	NA	NA
		16001	160058	Binder	Floor	Calcite	396	72
	5	11046	110248	Binder	Floor	Calcite	335	53
		11046	110248	Binder	Floor	Calcite	356	78
		11046	110248	Binder	Floor	Calcite	362	81
		11046	110664	Binder	Floor	Calcite	405	95
		11148	110249	Binder	Floor	Calcite	380	84
		11234	110665	Binder	Floor	Calcite	384	75
		11046	110248	Aggregate	Floor	Aragonite	NA	NA
		11046	110248	Aggregate	Floor	Aragonite	NA	NA
		11046	110248	Aggregate	Floor	Aragonite	NA	NA
		11046	110664	Aggregate	Floor	Aragonite	NA	NA
		11234	110665	Aggregate	Floor	Aragonite	NA	NA
		11148	110249	Aggregate	Floor	Aragonite	NA	NA
	7	11152	110250	Binder	Wall	Calcite	406	105
		11152	110250	Aggregate	Wall	Aragonite	NA	NA
	8	11111	110251	Binder	Floor	Calcite	334	71
		11111	110251	Binder	Floor	Calcite	360	73
		11111	110251	Aggregate	Floor	Aragonite	NA	NA

Results and Discussion

The visual examination identified morphological differences between the plaster of the trading floors and that of the collecting vats: in the treading floors the plaster has a multilayered structure, whereas in the vats the plaster has only one or two thick layers of plaster. A microscopic examination of one sample from a treading floor revealed the stacked thin layers of plaster, which vary in thickness between 3.5 and 7.5 mm (Fig. 2).

The spectroscopic (FTIR) study, used to further study the composition of plaster, showed that all of the samples—both from the treading floors and the vats—contained calcite-based binders (lime) and shell aggregates (Table 1). The calcite base of the binders was identified by the IR peak positions (Fig. 3; Weiner, 2010: 284): 1421 (V3 vibrational band), 875 (V2 vibrational band) and 712 cm^{-1} (V4

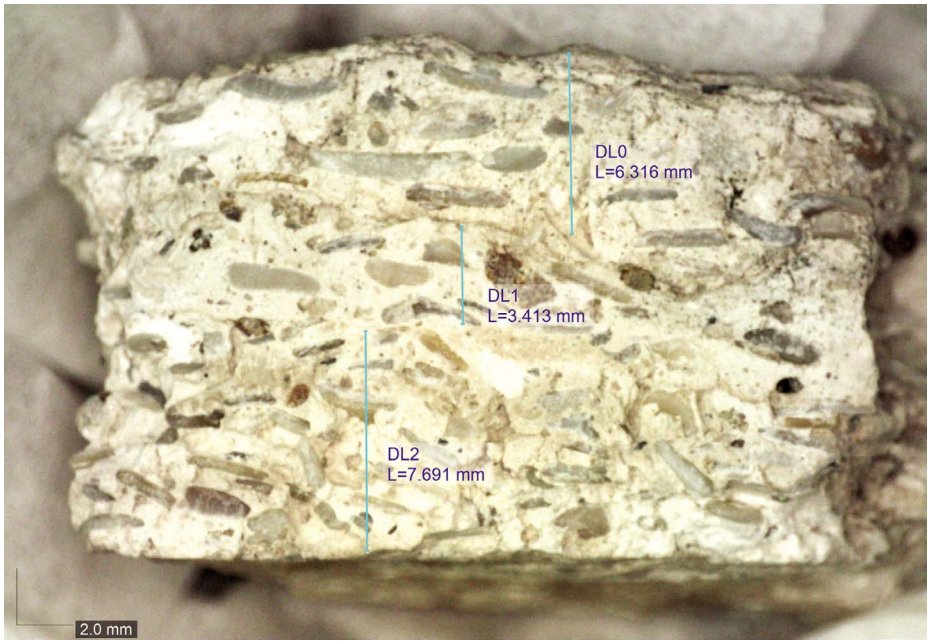

Fig. 2. A representative cross-section of a plaster sample with shell aggregates (sample L11046, B110248).

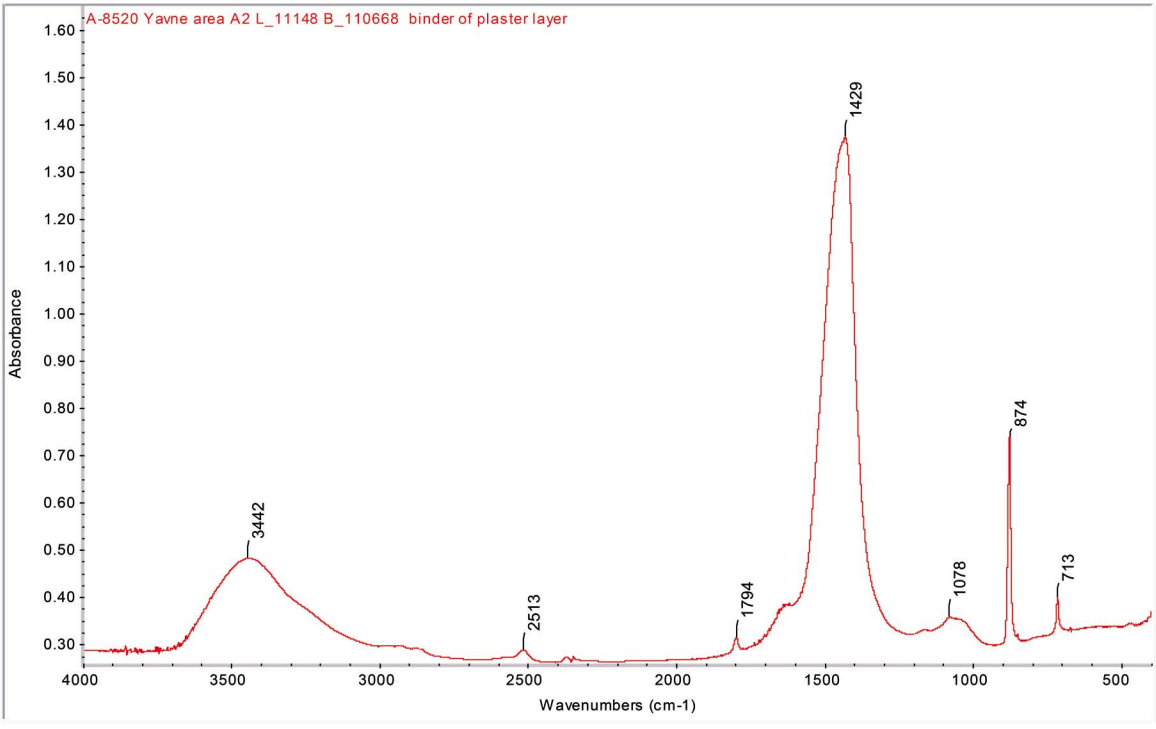

Fig. 3. FTIR spectra of a representative binder sample (L11148, B110668);

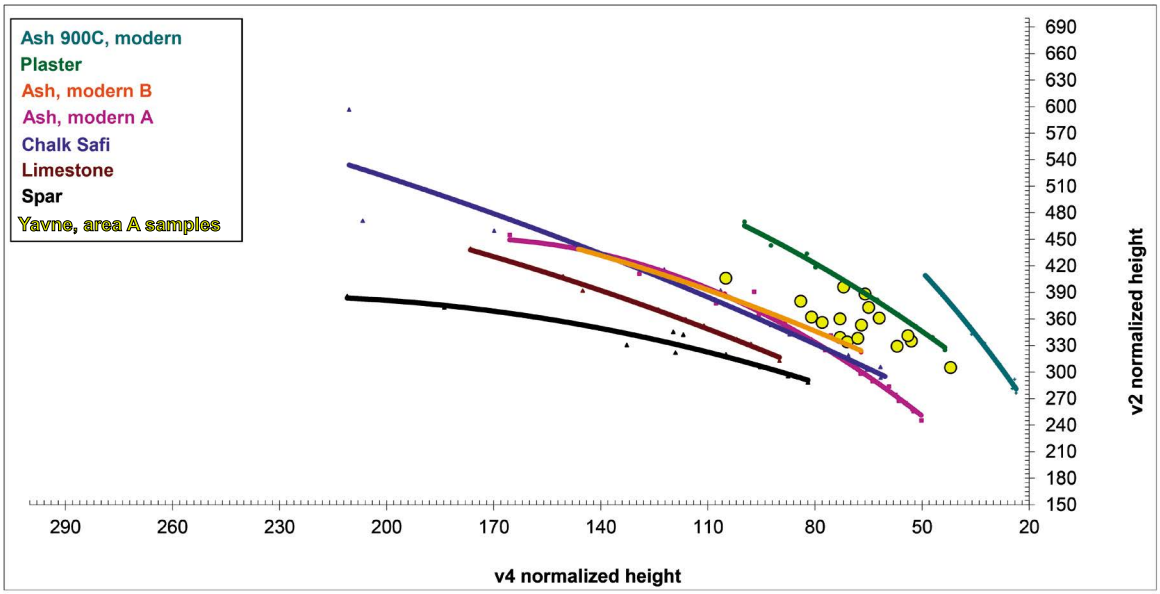

Fig. 4. Calcite Grinding Curve and Area A samples (following Regev et al. 2010).

vibrational band). Another peak that was found in all binder spectra appeared within the range of 1038 to 1083 cm^{-1}. This peak represents the silicate family, which is associated with clay or quartz; due to their small amount, these were obviously contaminations.

When plotting the FTIR analysis of the binders into the grinding curve presented in Regev et al. (2010) all the samples show atomic disorder between the curve of the modern plaster (highly disordered) and that of chalk (geological ordered material). This is an indication that the samples come from relatively well-preserved plasters, with minimal influence from geological materials—corroborating the microscopic analysis—and that the binder was slightly recrystallized (Fig. 4).

The shell fragments comprising the aggregates are small and rounded and do not exhibit any fresh breaks, suggesting that they were rounded naturally by erosion from water flow and purposely collected for this quality. Shells are composed of the mineral aragonite, which is a carbonate having the identical chemical composition of calcite but with a different atomic configuration. Most of the aggregate samples were identified as aragonite by peaks at 1476 (V3), 857 (V2) and 712 (V4) cm^{-1} (Fig. 5).

As aragonite is slightly less thermally stable than calcite, this composition allows us to learn about the technology by which the plaster was produced. The presence of aragonite suggests that none or only little heating of the shells was involved in the process of preparing the plaster, as aragonite converts into calcite when heated around 400°C. Interestingly, one sample, from Collecting Vat D, yielded a different result: calcite shell aggregate. This indicates that the shells were heated to a temperature of 400°C or more before they were mixed into the plaster, since the plaster did not bear any visual signs of heating, such as black soot.

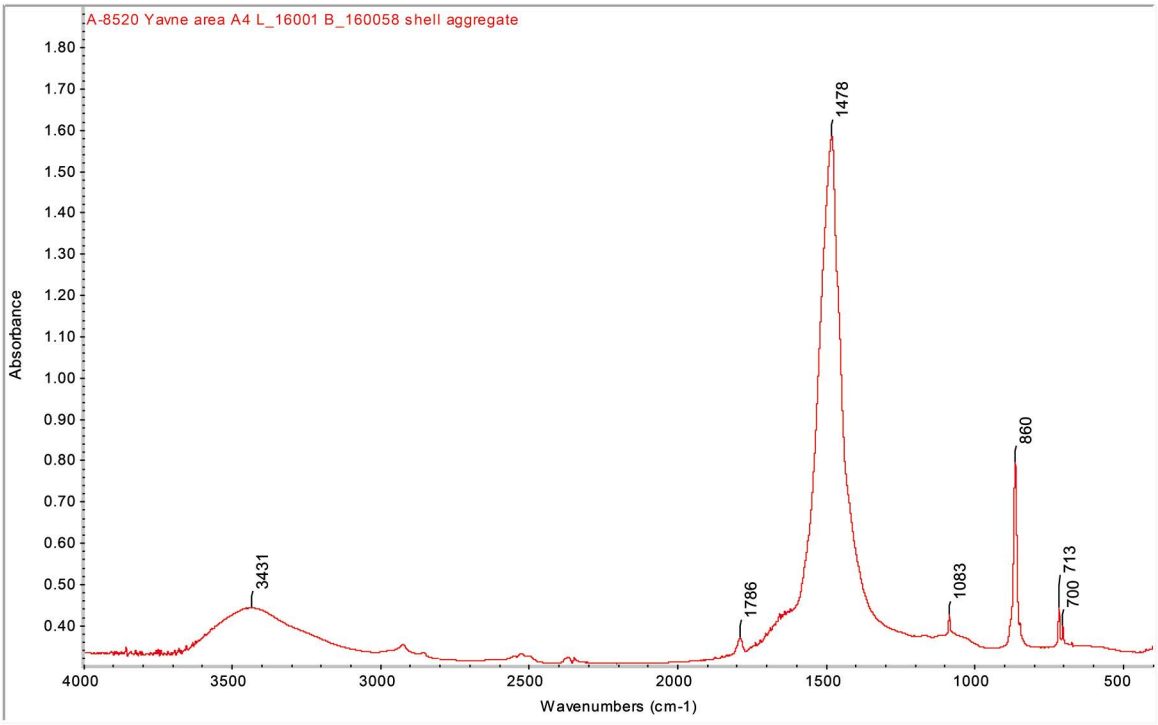

Fig. 5. FTIR spectra of a shell aggregate sample (L11148, B110249);
aragonite peak position: 1474, 858, 713.

CONCLUSIONS

The study identified morphological differences between the plaster of the treading floors and that of the collecting vats, which probably reflect the differences in function between these installations. Furthermore, preliminary results point to compositional similarities of both the binder and the aggregates of the plaster samples from the various types of vats, suggesting that despite their typological differences they served a similar function. By using the grinding curve method, the plaster samples show that their binder is well preserved, and that aggregates were mostly unburned shells. One sample, of the shell aggregate from Vat D, indicates that it was exposed to heat. This observed difference in the treatment of the aggregate suggests a possible difference in technology or use.

References

Asscher Y. and Goren Y. 2016. A Rapid On-Site Method for Micromorphological Block Impregnation and Thin Section Preparation. *Geoarchaeology* 31/4:324–331.

Chu V., Regev L., Weiner S. and Boaretto E. 2008. Differentiating between Anthropogenic Calcite in Plaster, Ash and Natural Calcite Using Infrared Spectroscopy: Implications in Archaeology. *JAS* 35:905–911.

Poduska K.M., Regev L., Boaretto E., Addadi L., Weiner S., Kronik L. and Curtarolo S. 2011. Decoupling Local Disorder and Optical Effects in Infrared Spectra: Differentiating between Calcites with Different Origins. *Advanced Materials* 23:550–554.

Regev L., Poduska K.M., Addadi L., Weiner S. and Boaretto E. 2010. Distinguishing between Calcites Formed by Different Mechanisms Using Infrared Spectrometry: Archaeological Applications. *JAS* 37:3022–3029.

Weiner S. 2010. *Microarchaeology: Beyond the Visible Archaeological Record*. Cambridge.